

SAFETY ASSESSMENT FOR LOCA IN CANDU REACTOR LOADED WITH CANFLEX-NU FUEL BUNDLES

Dirk J. Oh, Myeong Y. Ohn*, Kang M. Lee**, Ho C. Suk

Korea Atomic Energy Research Institute

Advanced Heavy Water Reactor Fuel Development Division

P.O. Box 105, Yusong, Taejeon, Korea 305-600

(* Present Address: Korea Power Engineering Company,

** Present Address: Korea Nuclear Fuel Company)

Joseph H. Lau

AECL CANDU

Fuel Design Branch

2251 Speakman Drive, Mississauga, Ontario L5K 1B2, Canada

1. INTRODUCTION

Currently, the Korea Atomic Energy Research Institute (KAERI) and Atomic Energy of Canada Limited (AECL) are jointly developing an advanced Canada deuterium uranium (CANDU) fuel, called CANDU Flexible Fuelling (CANFLEX). The CANFLEX 43-element bundle design has two major design improvements over the standard CANDU-6 37-element bundle while maintaining compatibility with the existing CANDU reactor fuel-handling systems and all other fuel performance characteristics. First, the CANFLEX bundle contains 43 elements of two different diameters, thereby reducing peak linear element power by 20% (i.e., < 50 kW/m), as shown in Figure 1. The lower linear element power not only enables a 200% increase in average discharge burnup (i.e., 21000 MWD/MTU) with the use of slightly enriched uranium compared with the standard natural uranium bundle but also improves the safety margins of CANDU reactors. Second, the CANFLEX bundle has the attachment of critical heat flux enhancement pads called buttons. The buttons increase critical channel power by about 5%, which leads to the improvement of the operating margins for CANDU reactors.

This paper describes the safety assessment results for the two representative large-break LOCAs in CANDU-6 reactor loaded with CANFLEX-natural uranium (NU) fuel bundles; 35% reactor inlet header (RIH) break and 100% reactor outlet header (ROH) break. The 35% RIH and 100% ROH breaks are chosen because they are limiting accidents for fuel channel integrity and fission product release (FPR)

standpoints, respectively (Reference 1). The predicted results are compared with those for the reactor loaded with standard 37-element bundles.

2. ANALYSIS METHODOLOGY

2.1 Methodology for Fuel Channel Integrity Analysis

The CATHENA two fluid thermalhydraulic code (Reference 2) is used for fuel channel analysis. The response of the heat transport system to the 35% RIIH break for a CANDU-6 reactor is analyzed using a CATHENA "full circuit" model. The effects of individual channel characteristics (elevation, feeder geometry, channel power, etc.) on fuel and fuel channel behaviour are analyzed by way of "slave" single channel simulations using header boundary conditions predicted by the full circuit simulations. The CATHENA slave channel (Reference 3) contains a more detailed model for fuel and PT than the full circuit model. A node-link model of the fuel channel assembly is constructed and the transient thermalhydraulic header boundary conditions (pressure, enthalpy and void fraction) from the full-circuit simulations are applied to the inlet and outlet headers.

Figures 2 and 3 illustrate the CATHENA fuel and fuel channel models using a 43-element CANFLEX and a 37-element standard fuel bundle cross section, respectively. The model provides a detailed nodalization of the fuel bundle, pressure tube and calandria tube. The CANFLEX bundle (Figure 2) consists of 43 fuel elements arranged in four rings (21, 14, 7 and 1 in the outer, intermediate, inner and center elements, respectively), while the standard bundle (Figure 3) consists of 37 fuel elements arranged in four rings (18, 12, 6 and 1 in the outer, intermediate, inner and center elements, respectively). Each element (except the center and top element) is circumferentially divided into two sectors primarily to capture the different "inside" and "outside" surface temperatures for the thermal radiation calculation. The center element has one sector while the top element has 16 and 18 sectors for the CANFLEX and standard bundles, respectively. Both the PT and CT are divided into 32 circumferential sectors. The numbers in Figures 2 and 3 indicate the sector numbering schemes for the thermal radiation calculation.

A high powered channel O6 is selected for the analysis. The fuel channel is divided axially into 12 nodes corresponding to the 12 fuel bundles. Both the maximum channel and bundle powers (bundles 6 and 7) of channel O6 are normalized to the maximum operating limits of 7.3 MW and 935 kW, respectively.

2.2 Methodology for FPR Assessment

The methodology to determine FPR for a postulated large LOCA is detailed in Reference 1. The methodology is briefly described in this section.

FPR estimate is obtained by determining which fuel elements are expected to fail following the accident and their times of failure. The inventories of FPR following the accident are estimated to be equal to the gap inventories of the failed fuel elements plus 1% of the grain-bound inventories of the failed fuel elements in the critical core pass. The latter inventories are added to the former to account for the possibility of additional releases of fission products from the fuel matrix due to diffusion, oxidation, Zircaloy-UO₂ interaction and UO₂ cracking.

The analysis is composed of four parts: (i) estimate of fission product inventories and distribution in the fuel elements in the reactor core at the time of the accident; (ii) estimate of fuel element failure thresholds of linear power at various burnups; (iii) estimate of the number of fuel elements expected to fail and their times of failure, and; (iv) estimate of the transient FPR from failed fuel elements.

ELESTRES (Reference 4) simulations using the ANS 5.4 gas release model (Reference 5) generate a list of the total and gap inventories for the complete operating ranges of fuel element linear power between 5 kW/m and 61 kW/m, and burnup between 10 MW.h/kg(U) and 240 MW.h/kg(U).

The fuel failure thresholds are defined as follows: for a given burnup, the fuel failure threshold is the maximum linear power (in kW/m) which would result in a prediction of fuel element not failing following a large LOCA. The fuel failure thresholds are determined for fuel element burnups ranging from 10 MW.h/kg(U) to 240 MW.h/kg(U) using the ELESTRES and ELOCA (Reference 6) computer codes. The transient thermalhydraulic boundary conditions from the CATHENA slave channel simulations for a fuel element in the outer ring at the top of bundle 6 (935 kW) of the O6 channel (7.3 MW) are used in the ELOCA simulations to calculate the fuel failure thresholds.

Simple and conservative criteria are used to determine whether a fuel element fails or not, based on the predictions of the ELOCA code. These criteria are based on experimental data and experience with operating reactors. The criteria used here are listed below.

The fuel sheath is considered to remain intact if the following are satisfied:

1. No fuel centerline melting. A fuel element will be assumed to fail if centerline melting (2840 °C) is reached, due to volume expansion causing excessive sheath strain.
2. No excessive diametral strain. The uniform sheath strain shall remain less than 5 percent for sheath temperatures lower than 1000 °C (References 7 and 8).
3. No significant cracks in the surface oxide. The uniform sheath strain shall remain less than 2 percent for sheath temperatures higher than 1000 °C (Reference 9).
4. No oxygen embrittlement. Oxygen concentration shall remain less than 0.7 weight percent over half the sheath thickness (Reference 10).
5. No sheath failure by beryllium-braze penetration at bearing pad and spacer pad locations (Reference 11).

The number of fuel elements expected to fail is estimated by adding the number of fuel elements in each power/burnup group where the power is equal to or greater than the fuel failure threshold at that burnup.

For each power/burnup group considered as failed, the timing of fuel failure is estimated, based on the corresponding ELOCA predictions.

3. ANALYSIS RESULTS

3.1 Fuel Channel Integrity Analysis Results for 35% RIH Break

Figure 4 shows the relative channel power histories obtained from the power pulse analysis for the 35% RIH break for each CANDU-6 reactor loaded with either the CANFLEX or standard bundles. The power pulses have integrated powers of 4.2 and 3.8 full power seconds (FPS) up to 3 seconds from the start of the accident for the CANFLEX and standard bundle cases, respectively. The 0.4 FPS higher integrated power of the CANFLEX bundle case is due to the higher void reactivity of the CANFLEX bundle compared with the standard bundle case (Reference 12).

Transient thermalhydraulic header boundary conditions were obtained from the CATHENA full circuit analysis for the 35% RIH break for each CANDU-6 reactor loaded with either the CANFLEX or standard bundles. Both header boundary conditions are found to be very similar to each other because the CANFLEX bundles

are designed to be hydraulically compatible with the standard bundles.

The fuel channel coolant pressure and void fraction, and flow transients at axial node 7 are shown in Figures 5 and 6, respectively. The three hydraulic parameter transients for both bundle cases are almost the same, indicating both bundles are hydraulically nearly equivalent. After the break is initiated, the channel pressure decreases rapidly and the void fraction increases rapidly (Figure 5). The void fraction never quite reaches 1.0, indicating that a small amount of water is predicted to remain in the bottom of the channel. The initial rapid flow reversal is due to the break initiation. Through the competing forces of the break and the pump, the channel flow stagnates at 10 s and then reverses again at 17 s. The flow between 14 and 16 s is slightly negative, but relatively higher than the rest. The channel refills at about 91 and 87 s for the CANFLEX and standard bundles, respectively.

Figure 7 shows the temperature transients for the centerline, top and bottom sector sheath of the top fuel element (Sectors 51 and 44 in Figure 2, and Sectors 48 and 40 in Figure 3), the inside surface of the PT top sector (Sectors 67 and 64 in Figures 2 and 3, respectively) and the channel coolant at axial node 7. The fuel centerline temperature rapidly increases due to the short-lived power pulse (Figure 4) caused by the positive void coefficient of CANDU reactor. The maximum fuel centerline temperatures for the CANFLEX and standard bundles are 2025 and 2361 °C, respectively and both occur at 1.6 s. The sheath and coolant temperatures show similar behaviour; an initial rapid increase up to 10 s, a modest increase between 10 and 17 s except the sudden drop between 14 and 16 s, and a decrease afterward. The behaviour is very closely related to the aforementioned flow behaviour due to the strong flow velocity dependence of steam convective heat transfer in the stratified flow regime. The maximum bottom sector sheath temperatures for the CANFLEX and standard bundles are 1411 and 1506 °C, respectively and both occur at 18 s. However, the top sector sheath temperatures are lower compared to the bottom sector sheath because of the radiative heat transfer to the opposite cool PT. The maximum top sheath temperatures for the CANFLEX and standard bundles are 1259 and 1331 °C, and they occur at 18 and 16 s, respectively. The lower fuel centerline and sheath temperatures of the CANFLEX bundle in spite of the higher power pulse are attributed to the lower initial stored heat caused by the lower linear element power of the CANFLEX bundle as compared with the standard bundle.

The PT top sector temperature (Figure 7) monotonously increases up to the time of PT/CT contact and then rapidly cools down because of the heat loss to the surrounding moderator. The PT heatup rate for the CANFLEX bundle is lower

compared to the standard bundle. The PT contacts its CT at 21 and 19 s with the average contact temperatures and pressures of 811 and 812 °C and 3.9 and 4.0 MPa for the CANFLEX and standard bundles, respectively. The maximum PT top sector temperatures at the time of each PT/CT contact for the CANFLEX and standard bundles are 825 °C and 826 °C, respectively. The convective and radiative heat flux transients at the sheath outside and PT inside surfaces are shown in Figure 8. Figure 8 demonstrates that the lower PT heatup rate and temperatures of the CANFLEX bundle compared with those of the standard bundle are mainly due to the lower radiative heating by the lower temperature sheaths. The convective PT heating by coolant is almost similar for the both bundles as shown in Figure 8. The minimum top sector PT thicknesses at the end of the simulation (100 s) for the CANFLEX and standard bundles are 78% and 83% of the original PT thickness, respectively. The slightly thinner PT thickness (i.e., the slightly higher PT hoop creep strain) for the CANFLEX bundle is due to the about 2 s longer period of PT temperatures greater than the PT creep onset temperature 600 °C (Reference 13) as shown in Figure 7. The longer high PT temperature period for the CANFLEX bundle is mainly attributed to the 2 s later PT/CT contact.

Figure 9 shows the circumferential temperature distribution at 0, 5, 10, 15 and 19 s (the time of PT/CT contact for the standard bundle). The nearly flat temperature distribution for upper half part of PT is characteristic of a steam-exposed PT in a fully voided channel. For the thermalhydraulic temperature non-uniformities, no PT failure prior to PT/CT contact for both bundles was predicted based on Shewfelt's upper and lower bound failure criteria (Reference 14). Fuel channel integrity after PT/CT contact is also guaranteed for both bundles because moderator subcooling margin is enough to prevent CT dryout based on the results of contact boiling experiments (Reference 15). The 1 °C lower average PT/CT contact temperature for the CANFLEX bundle results in the negligible increase in the moderator subcooling margin.

3.2 FPR Assessment Results for 100% ROH Break

Figure 4 shows the relative channel power histories obtained from the power pulse analysis for the 100% RIH break for each CANDU-6 reactor loaded with either the CANFLEX or standard bundles. The power pulses have integrated powers of 4.2 and 3.9 full power seconds (FPS) up to 3 seconds from the start of the accident for the CANFLEX and standard bundle cases, respectively. The 0.3 FPS higher integrated power of the CANFLEX bundle case is due to the higher void reactivity of the CANFLEX bundle compared with the standard bundle case (Reference 12).

Figure 10 shows the fuel average and sheath temperature, and sheath strain transients for the outer elements of the bundle 6 (935 kW) at burnup of 60 MW.h/kg(U) from ELOCA simulations. The burnup of 60 MW.h/kg(U), also called the plutonium peak, is roughly the time when the fuel element's temperature is at a maximum during its residence in the reactor. The power/burnup history up to the burnup is assumed to be the limiting element power history shown in Figure 11. The temperatures for both bundles show similar behaviour; an initial rapid increase due to the short-lived power pulse, a decrease due to the flow increase following the pump recovery up to about 20 s, then a re-increase due to the late stagnation up to the first ECC refill times. The lower fuel average and sheath temperatures for the CANFLEX bundle in spite of the higher power pulse are attributed to the lower initial stored heat caused by the lower linear element power of the CANFLEX bundle as compared with the standard bundle. The sheath strains for the CANFLEX bundle case are lower than those for the standard bundle case due to the lower FPR (i.e. the lower internal gas pressure) and fuel/sheath temperatures of the CANFLEX bundle case, compared with the standard bundle case.

Figure 11 shows the fuel failure thresholds. The fuel failure thresholds for the CANFLEX and standard bundle elements are very similar because both bundles have the same fuel material (natural UO_2) and the nearly same sheath radius to thickness ratio, and undergo the nearly same hydraulic transients following the accident (i.e., the nearly same coolant pressure and sheath-to-coolant heat transfer coefficient transients). All the sheaths at the corresponding failure thresholds for the CANFLEX and standard bundles fail by criterion 3 in Section 2.2, except those for the CANFLEX inner elements at burnups of 220 to 240 MW.h/kg(U), which fail by criterion 4. The limiting power envelope for the CANFLEX bundle elements is lower than by about 10 kW/m than that for the standard bundle elements and the limiting power at each burnup for the CANFLEX bundle elements are always lower than the corresponding fuel failure threshold, as shown in Figure 11. Therefore, it is expected that almost no fuel failure will be observed for the CANFLEX bundle elements. Indeed, the fuel failure analysis predicts that the number of failed fuel elements for the CANFLEX bundle case is none, while that for the standard bundle case is 1827. The failed fuel elements for the standard bundle case belong to the outer ring of the high power bundles 4 to 9. The total (gap plus bound) I-131 releases for the CANFLEX and standard bundles are none and 5889 TBq, respectively. The significant reduction of the number of failed fuel elements and FPR for the CANFLEX fuel bundle is attributed to the lower linear power of the CANFLEX fuel bundle, compared with the standard fuel bundle.

4. SUMMARY & CONCLUSIONS

Fuel channel integrity and FPR analyses have been performed for LOCA in CANDU-6 reactor loaded with CANFLEX-natural uranium (NU) fuel bundles. The 35% RIH and 100% ROH breaks are chosen for fuel channel integrity and FPR analyses, respectively. The predicted results are compared with those for the reactor loaded with standard 37-element bundles.

The maximum fuel centerline and sheath temperatures of the full CANFLEX bundle channel for 35% RIH breaks were lower by 336 and 95 °C, respectively, than those for the standard bundle because of the lower linear power of the CANFLEX bundle in spite of the 11% higher power pulse of the CANFLEX bundle case. The PT/CT contact for the CANFLEX bundle occurred 2 s later than that for the standard bundle. The PT/CT contact temperature for the CANFLEX bundle was 1 °C lower than that for the standard bundle. These provide the CANFLEX bundle with the negligibly enhanced safety margin for the fuel channel integrity in CANDU 6 reactor, compared with the standard bundle.

The fuel failure thresholds for the CANFLEX and standard bundle elements are very similar. The fuel failure analysis predicts that the number of failed fuel elements for the CANFLEX bundle case is none, while that for the standard bundle case is 1827. The total (gap plus bound) I-131 releases for the CANFLEX and standard bundles are none and 5889 TBq, respectively. The significant reduction of the number of failed fuel elements and FPR for the CANFLEX fuel bundle is attributed to the lower linear power of the CANFLEX fuel bundle compared with the standard fuel bundle.

5. REFERENCES

1. S. Lam et. al., "Large Loss of Coolant Accident", 86-03500-AR-029 Rev. 1, August 1994.
2. D. J. Richards, "Validation of CATHENA Two-Fluid Code", Third International Topical Meeting on Reactor Thermalhydraulics and Operations, Seoul, Korea, November 14-17, 1988.
3. D. J. Oh, H. S. Lim, M. Y. Ohn, K. M. Lee and H. C. Suk, "Fuel Channel Analysis for a Large Break LOCA in a CANDU Reactor Loaded with CANFLEX Fuel Bundles", Nuclear Technology, 114, 292 (1996).
4. M. Tayal, "Modelling CANDU Fuel under Normal Operating Conditions: ELESTRES Code Description", AECL-9331, 1987, "Users' Manual for the M11C Version of the ELESTRES Code" TTR-234A, February 1989.

5. American National Standard Method for Calculating the Fractional Release of Volatile Fission Products from Oxide Fuel, ANSI/ANS-5.4-1982.
6. J.A. Walsworth and H.E. Sills, "High Temperature Transient Fuel Performance Modelling, ELOCA.MK4", AECL Research Report, CRNL-2010-1, 1984.
7. AECL (M.R. Matthias) Submission to AECCB (J.P. Marchildon, B.M. Ewing) with Attachment by E. Kohn, "Use of 5 Percent Uniform Strain for Activity Release Predictions", March 1, 1982.
8. C.E.L. Hunt, "The Limit of Uniform Strain, or Onset of Ballooning, in Fuel Sheath Ballooning Tests", AECL Report CRNL-1187, September 1974.
9. S. Sagat et al, "Deformation and Failure C.E.L. Hunt, "The Limit of Uniform Strain, or Onset of Ballooning, in Fuel Sheath Ballooning Tests", AECL Report CRNL-1187, September 1974.
10. A. Sawatzky, "A Proposed Criterion for the Oxygen Embrittlement of Zircaloy-4 Cladding", Zirconium in the Nuclear Industry (Fourth Conference), ASTM STP 681, pp. 479-496, 1979.
11. E. Kohn and S. Sagat, "Beryllium Assisted Cracking of Zircaloy", Sixth Canadian Fracture Conference, Harrison Hot Springs, B.C., Canada, June 1982.
12. H. C. Suk et. al., "Design and Analysis of CANDU Advanced Fuel", KAERI/RR-1624/95, July 1996.
13. R. S. W. Shewfelt, L. W. Lyall and D. P. Godin, "A High Temperature Creep Model for Zr-2.5 wt% Nb Pressure Tubes", J. Nucl. Mat., 125, 228 (1984).
14. R. S. W. Shewfelt and D. P. Godin, "Verification Tests for GRAD, a Computer Program to Predict the Non-uniform Deformation and Failure of Zr-2.5 wt% Nb Pressure Tubes During a Postulated Loss-of Coolant Accident", AECL-8384, Atomic Energy of Canada Limited (1985).
15. G. E. Gillespie, R. G. Moyer and P. D. Thompson, "Moderator Boiling on the External Surface of a Calandria Tube in a CANDU Reactor During a Loss-of-Coolant Accident", AECL-7664, Atomic Energy of Canada Limited (1982).

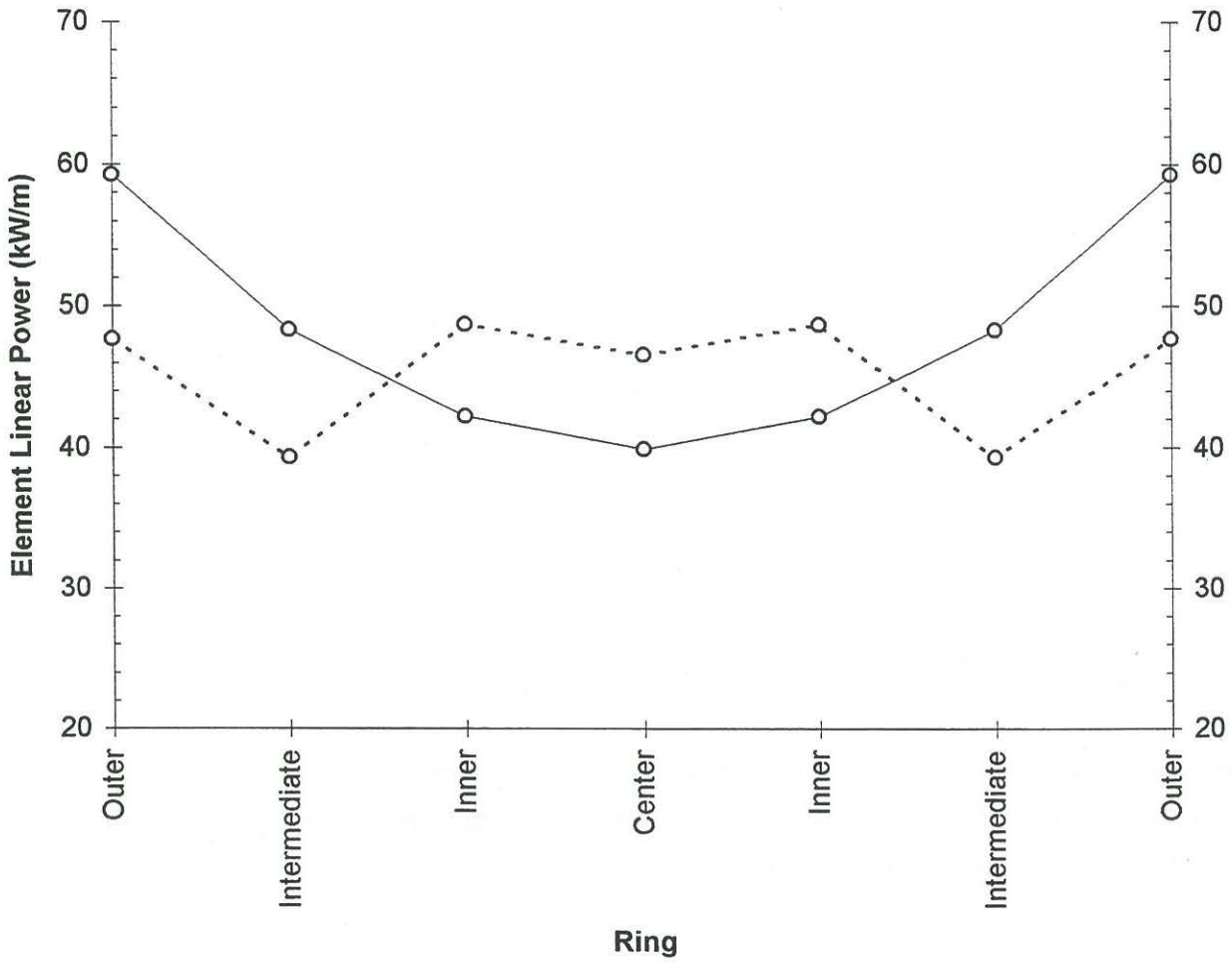


Figure 1: Element Linear Power for Each Ring of 935 kW Bundle at Plutonium Peak (60 MW.h/kgU); CANFLEX (solid line) & Standard (dotted line) Bundles

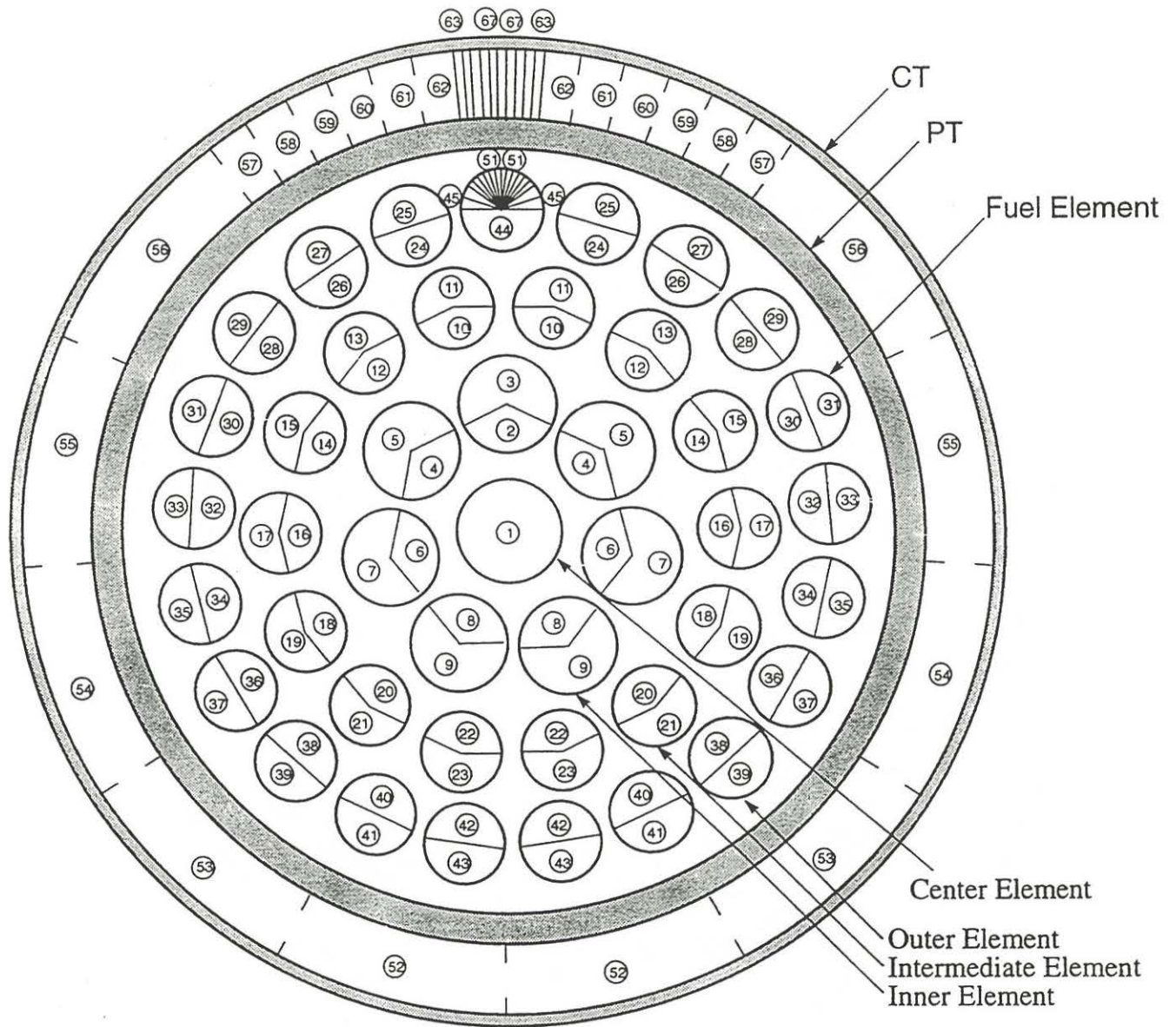


Figure 2. Sectoring of Fuel Channel in CANFLEX CATHENA Model

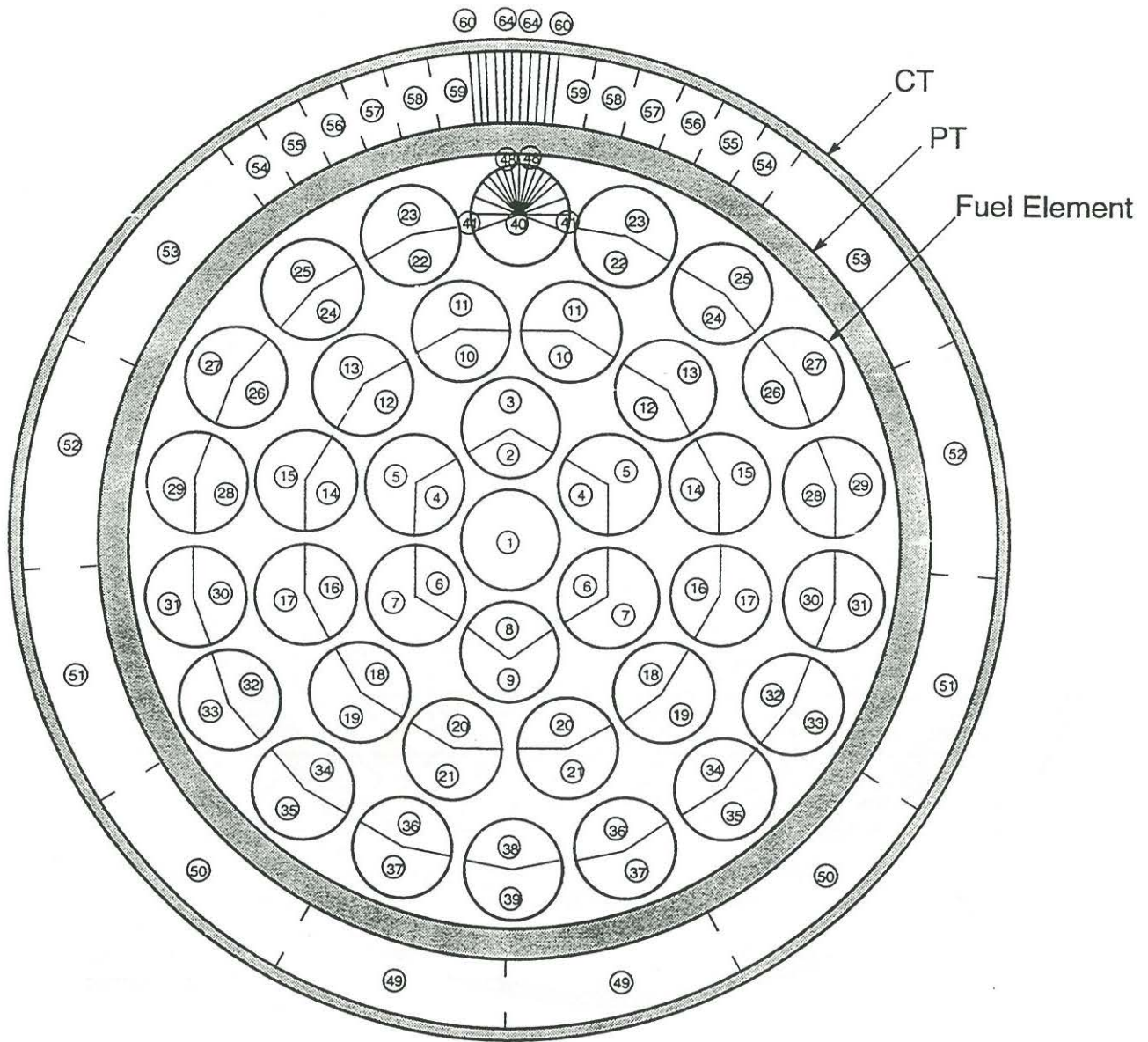


Figure 3. Sectoring of Fuel Channel in Standard CATHENA Model

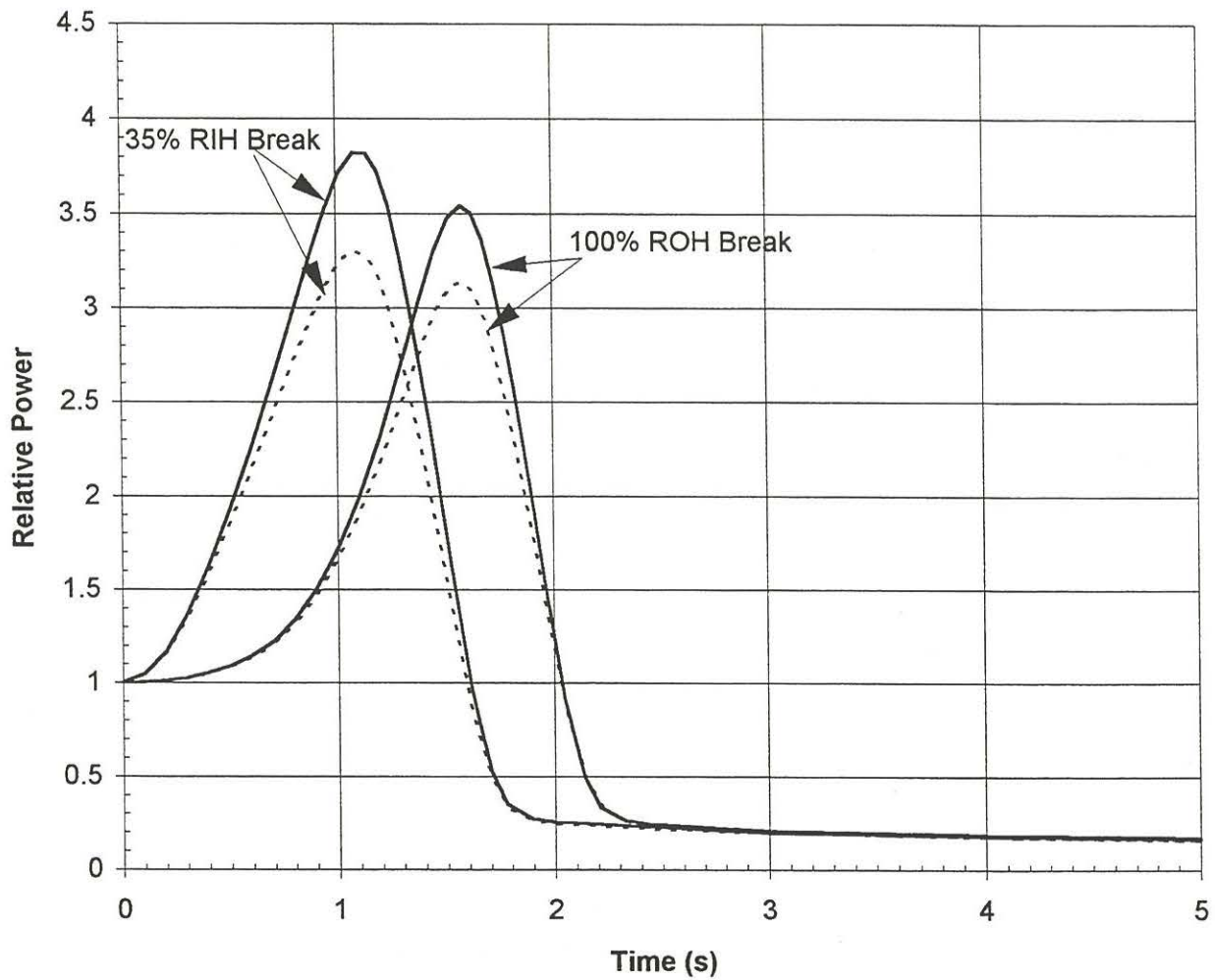


Figure 4. Power Pulses of O6 Channel for 35% RIH & 100 % ROH Breaks; CANFLEX (solid line) & Standard (dotted line) Bundles

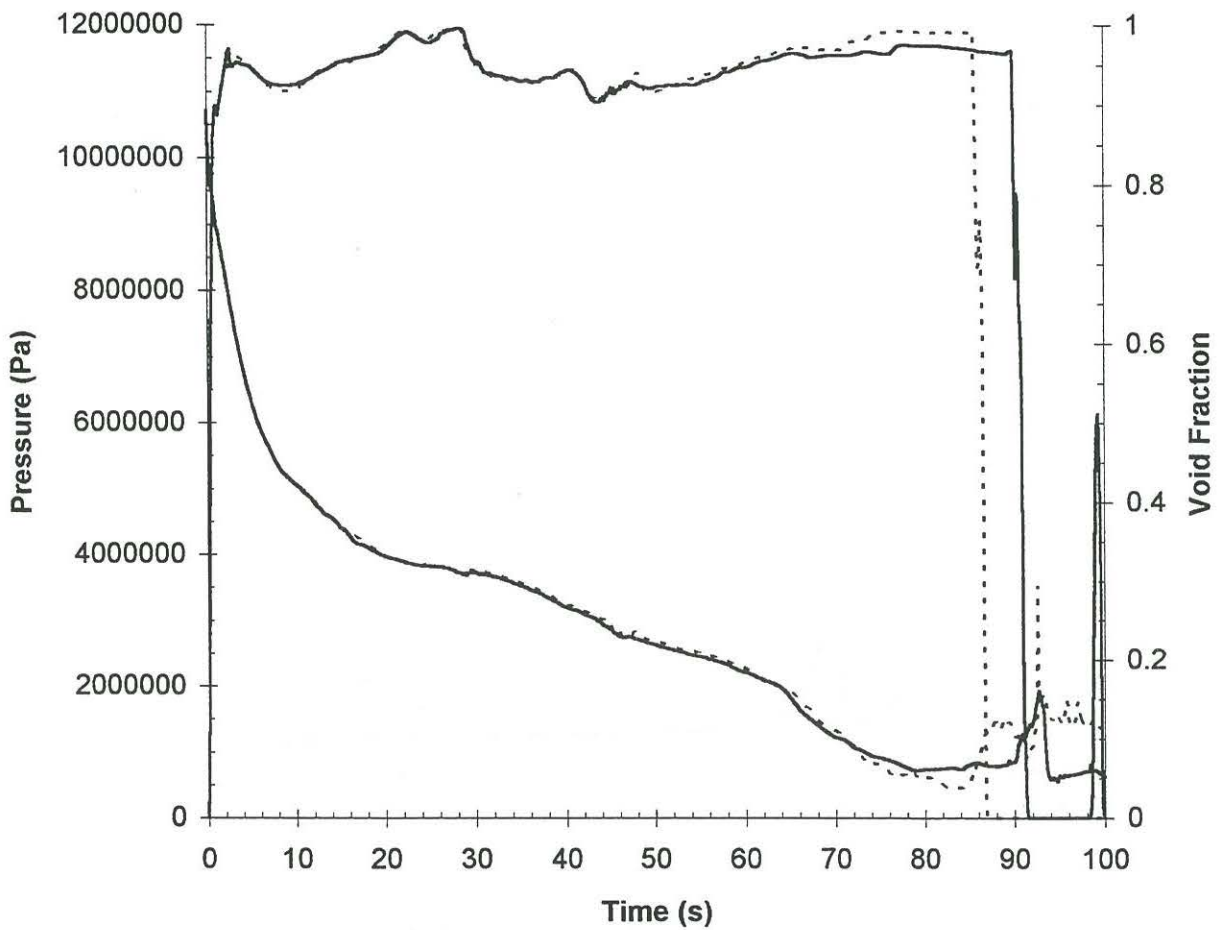


Figure 5 : Pressure & Void Fraction Transients at Mid-Channel of 7.3 MW (O6) Channel for 35% RIH Break Case; CANFLEX (solid line) & Standard (dotted line) Bundles

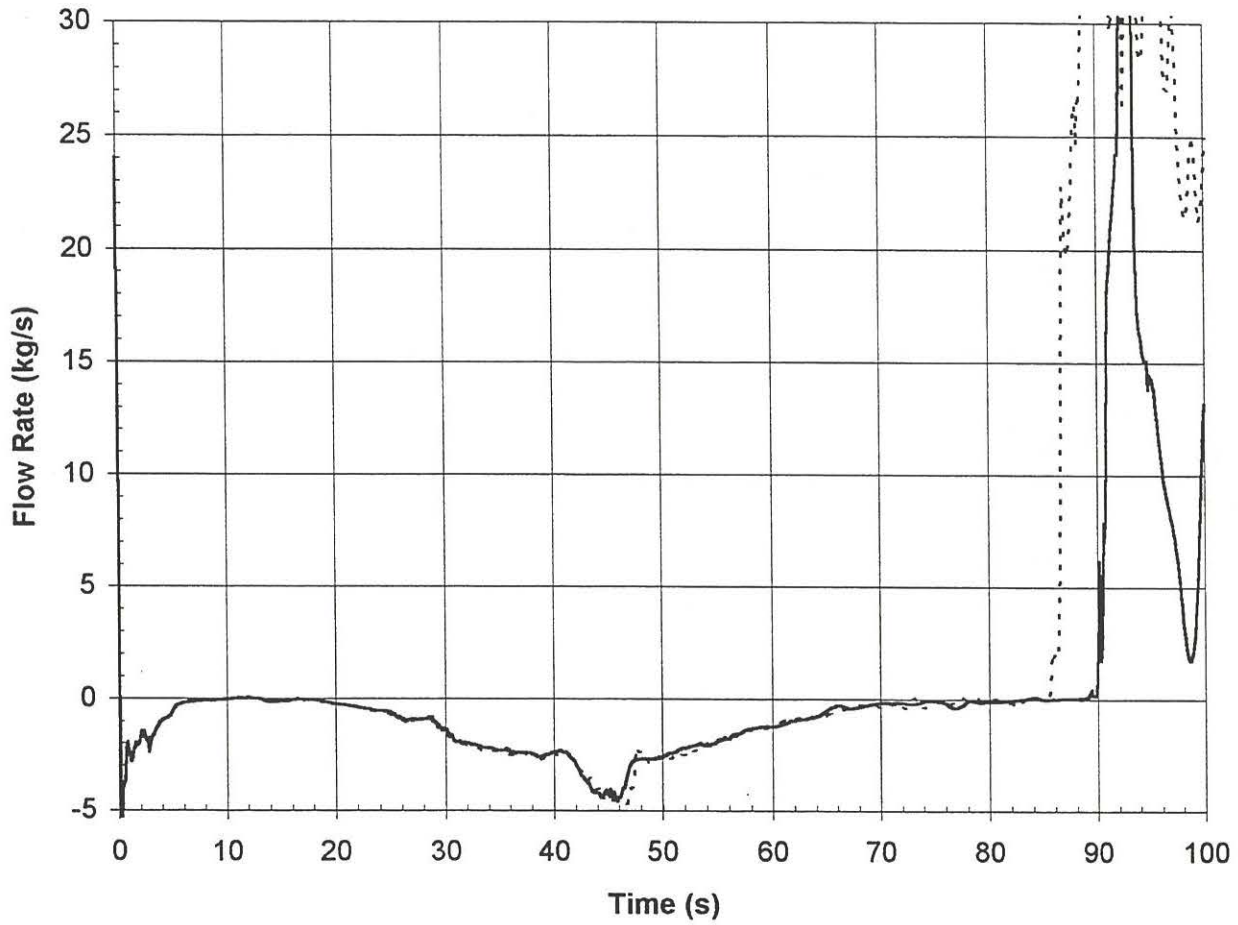


Figure 6 : Flow Transients at Mid-Channel of 7.3 MW (O6) Channel for 35% RIH Break Case; CANFLEX (solid line) & Standard (dotted line) Bundles

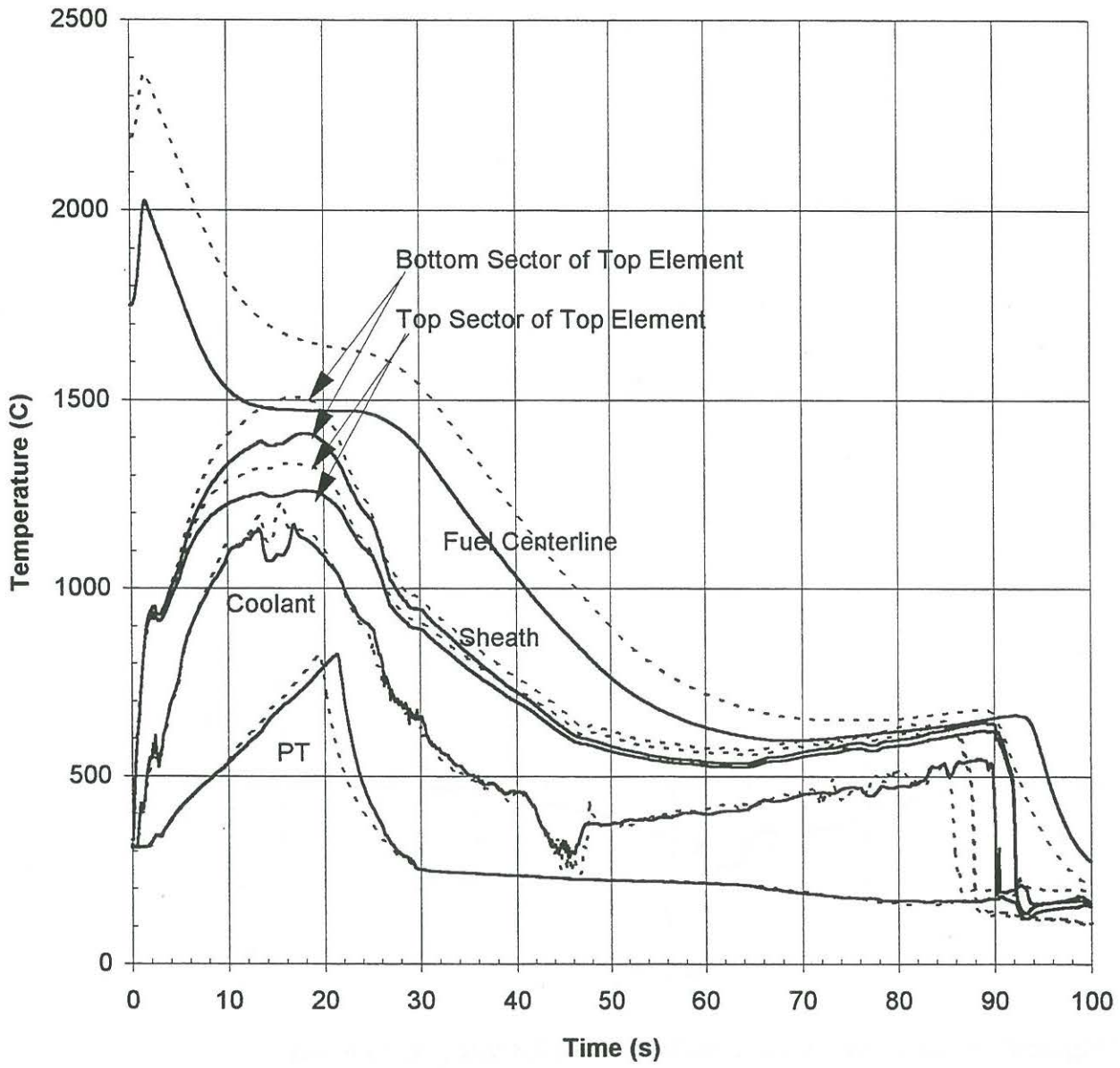


Figure 7. Temperature Transients At Axial Node 7 of 7.3 MW (O6) Channel for 35% RIH Break; Fuel Centerline, Sheath & PT Temperatures at the Top of the CANFLEX (solid line) & Standard (dotted line) Bundles

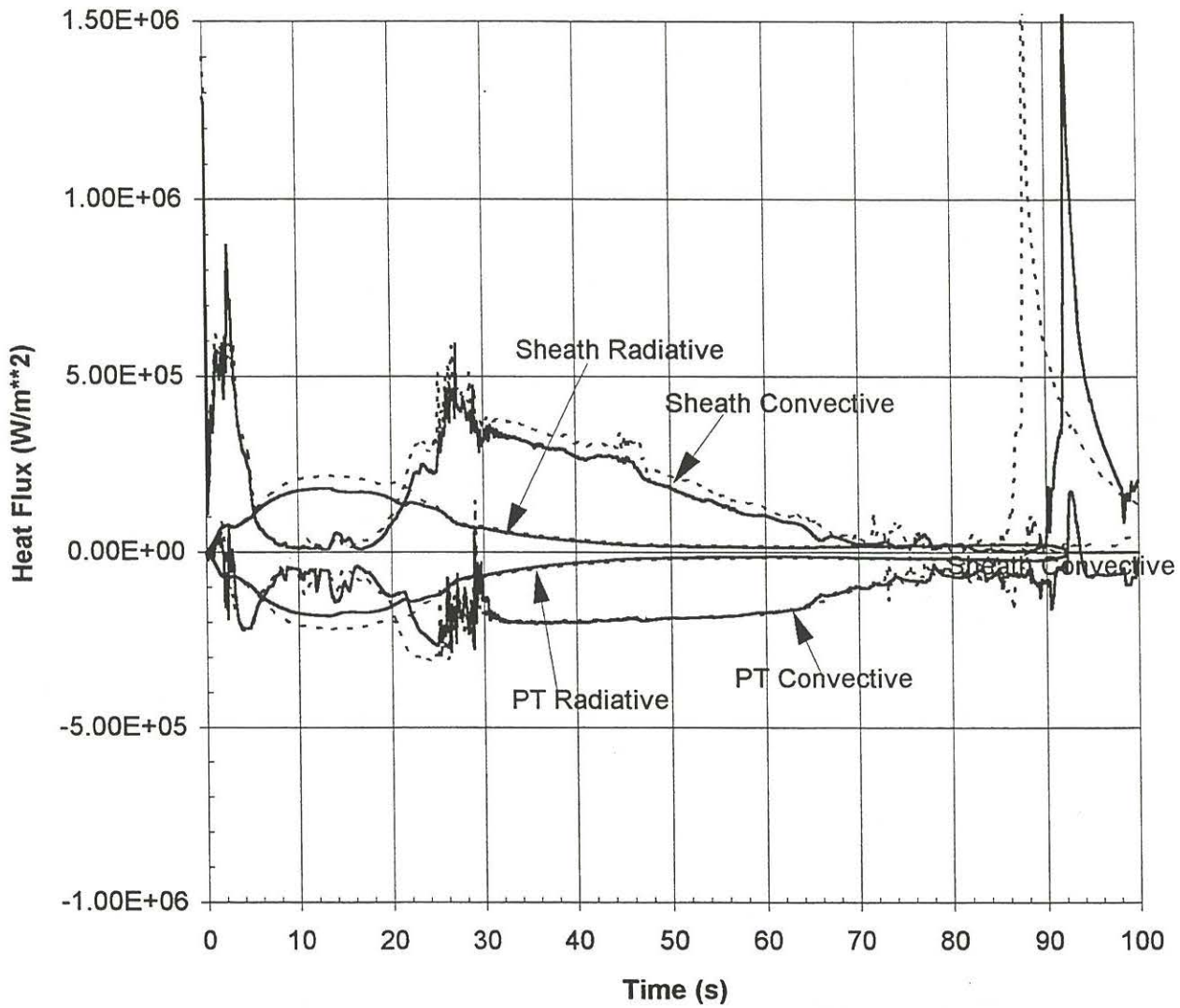


Figure 8. Heat Flux Transients at the Inside Surface of the PT Top Sector and the Top Sector of the Top Outer Element at Axial Node 7 of 7.3 MW (O6) Channel for CANFLEX (solid line) and Standard (dotted line) Bundles

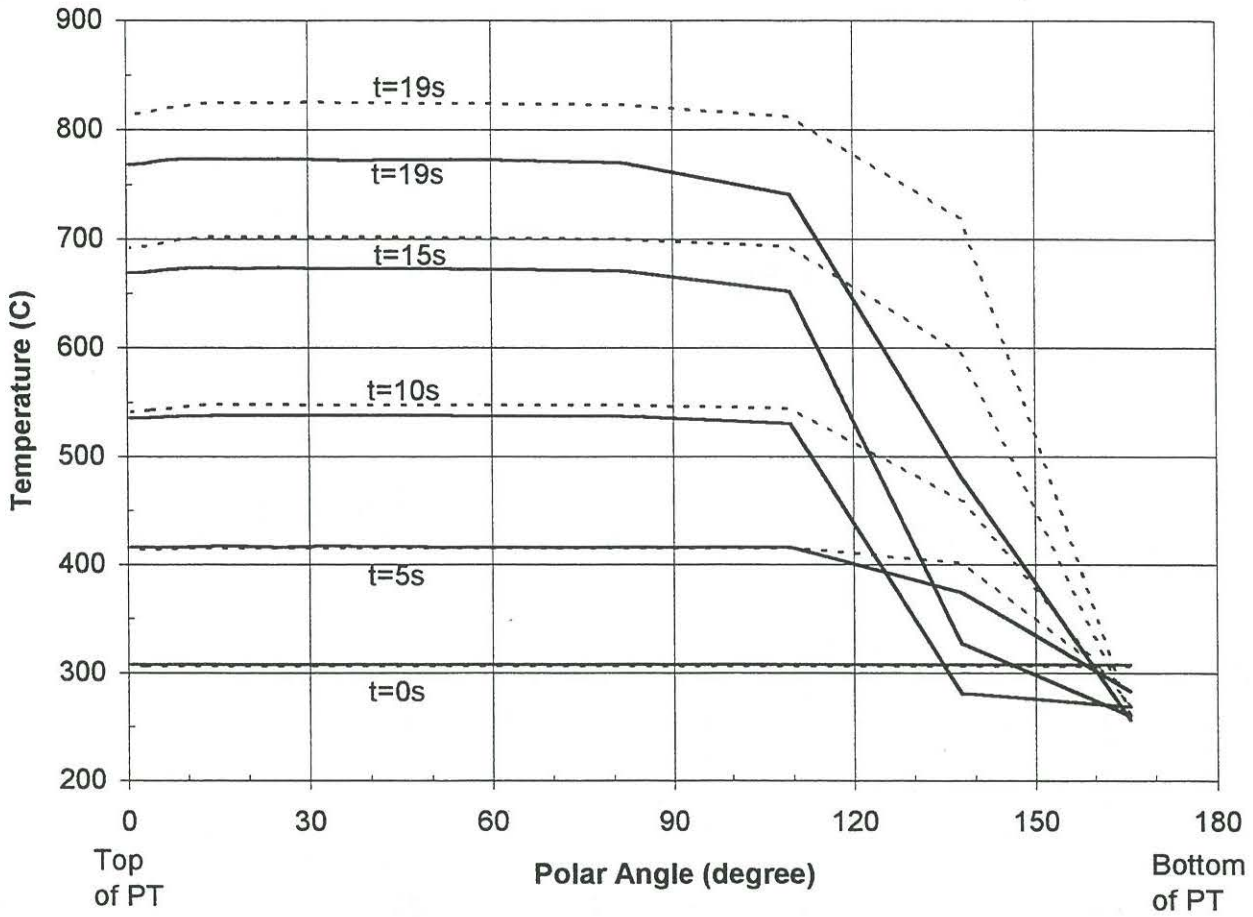


Figure 9. Circumferential PT Temperature Distribution At Axial Node 7 of 7.3 MW (O6) Channel for 35% RIH Break; CANFLEX (solid line) & Standard (dotted line) Bundles

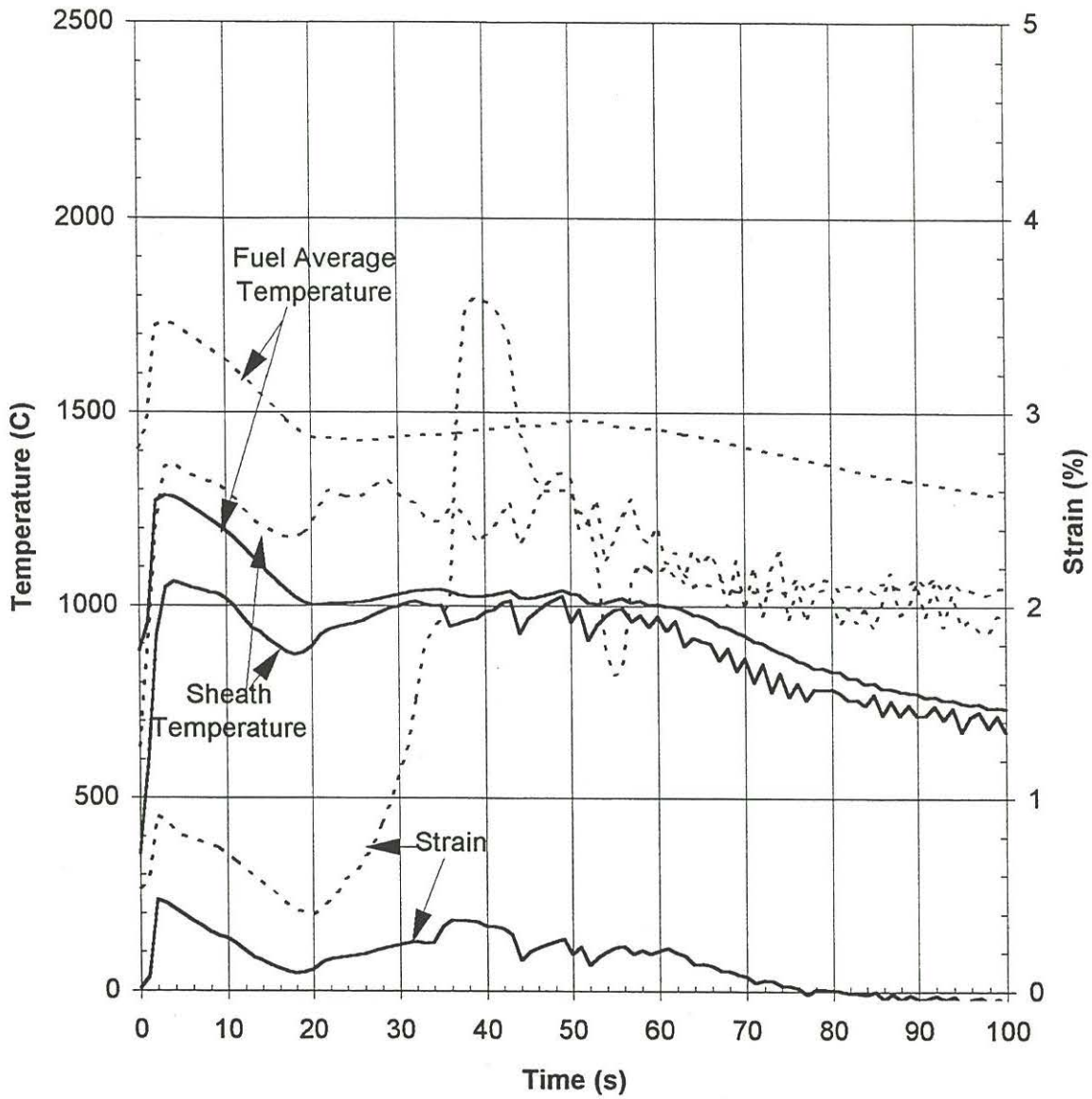
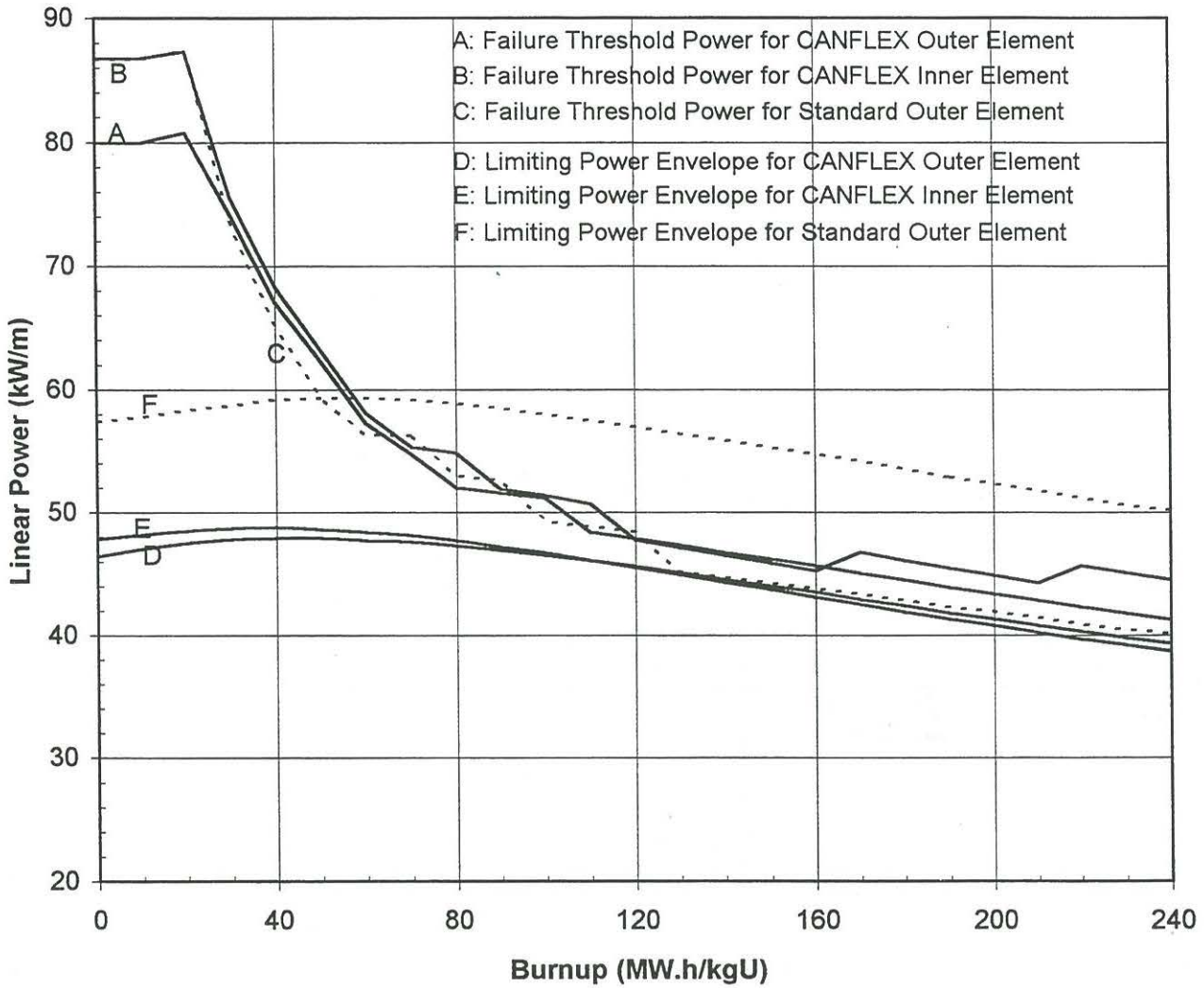


Figure 10. Temperature & Strain Transients for Outer Elements of Bundle 6 (935 kW) at Burnup of 60 MW.h/kg(U) for 100% ROH Break; the CANFLEX (solid line) & Standard (dotted line) Bundles



**Figure 11: Fuel Element Failure Thresholds for 100% ROH Break;
CANFLEX (solid line) & Standard 37-element Bundles**